Available online at www.sciencedirect.com

ScienceDirect

Solid State Communications 144 (2007) 181–184

solid
state
communications

www.elsevier.com/locate/ssc

Photoluminescence of thin films $ZrO_2:Er^{3+}$ excited by soft X-ray

Lee-Jene Lai[a,*], Tieh-Chi Chu[b], Meng-I Lin[c], Yao-Kwang Lin[a]

[a] *National Synchrotron Radiation Research Center, 101 Hsin-Ann Road, Hsinchu Science Park, Hsinchu 30077, Taiwan*
[b] *Department of Radiological Technology, Yuanpei Institute of Science and Technology, Hsinchu 30015, Taiwan*
[c] *Department of Nuclear Science, National Tsing Hua University, Hsinchu 30013, Taiwan*

Received 1 August 2007; accepted 29 August 2007 by P. Sheng
Available online 4 September 2007

Abstract

The photoluminescence (PL) properties and crystalline structure of undoped and erbium ion (Er^{3+})-doped zirconia (ZrO_2) that were prepared by sol–gel methods were examined. The ZrO_2 films exhibited a dopant concentration-dependent crystalline phase. As the Er^{3+} ions' concentration increases, the amount of monoclinic phases of ZrO_2 declines. However, the proportion of the tetragonal phase of ZrO_2 is enhanced. This fact suggests that Er^{3+} ions replace the Zr^{4+} ions and cause the phase transition in the host lattice of ZrO_2. Photoluminescence bands were observed by exciting the film at 300 eV with soft X-rays. Experimental results showed that the PL emission bands of Er^{+3}-doped ZrO_2 films can be tuned by controlling the Er^{3+} concentration. In particular, with increasing Er^{3+} concentration, the blue bands are quenched whereas the green and red bands are enhanced. This phenomenon can be explained as a non-radiative energy transfer.

PACS: 78.20.-e; 78.55.-m; 78.66.-w; 81.20.Fw

Keywords: A. Photoluminescence; B. Zirconia; C. Thin film; D. X-ray excitation

1. Introduction

Zirconia (ZrO_2)-based oxide ceramic is an excellent material because of its physical properties, which include its chemical stability, low thermal conductivity, low optical loss and high refractive index. This explains its use in a variety of applications, such as oxygen sensors, fuel cells and optically transparent materials [1–3]. Zirconia has three well-defined polymorphs, with monoclinic (ZrO_2/M), tetragonal (ZrO_2/T) and cubic (ZrO_2/C) phases. ZrO_2/M is thermodynamically stable up to 1100 °C; ZrO_2/T exists in the temperature range 1100–2370 °C, whereas ZrO_2/C is found above 2370 °C [4]. At room temperature, ZrO_2 exists in the monoclinic form since the cubic phase is metastable [5]. Furthermore, the optical properties of zirconia are modulated by the crystalline structure and by dopants [6,7]. Rare earth-doped luminescent thin films have emerged over the last few years, with potential applications in X-ray imaging systems and flat panel display devices [8–10]. Compared with the conventional powder phosphor display devices, the transparent thin-film phosphors are of greater interest due to their higher contrast and resolution, minimal optical scattering and better adhesion [10]. Er^{3+} ion-activated ZrO_2 is a promising candidate for making scintillator materials. Since its structure stabilization [11,12] has been used as a luminescence activator in monocrystalline zirconia and polycrystalline zirconia film, charge compensation associated with the substitution of Zr^{4+} by a trivalent ion, resulting in oxygen vacancies in the zirconia lattice, gives rise to the many optical properties of doped zirconia [13,14].

In this work, Er^{3+}-doped ZrO_2 thin films were prepared by a sol–gel method. The effect on the crystalline structure and optical properties of zirconia thin films by the variation of the Er^{3+} dopant concentration was investigated. Experimental results demonstrate that photoluminescence of ZrO_2 thin films is observed using soft X-ray excitation, also, the emission bands can be tuned by controlling the Er^{3+} concentration. The process conditions, consequent structures and luminescence properties of thin-film phosphors were reported in detail.

---

[*] Corresponding author. Tel.: +886 3 5780281; fax: +886 3 5783813.
E-mail address: jene@nsrrc.org.tw (L.-J. Lai).

0038-1098/$ - see front matter © 2007 Elsevier Ltd. All rights reserved.
doi:10.1016/j.ssc.2007.08.028

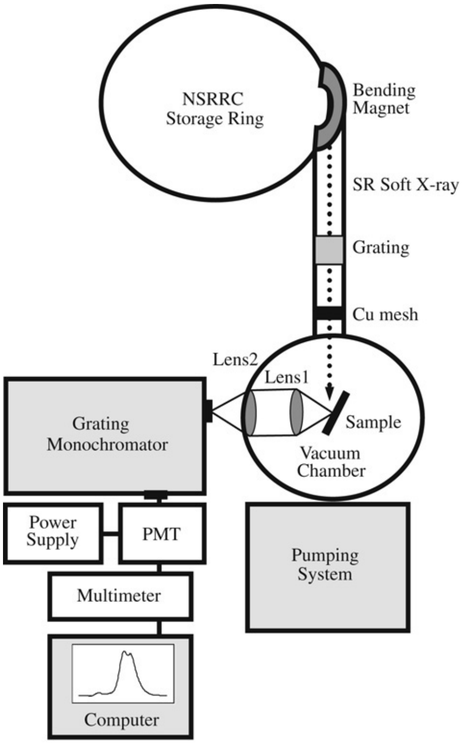

Fig. 1. Experimental setup for measuring soft X-ray-excited photoluminescence from ZrO_2 films doped with Er^{3+} ions on fused-silica substrates at NSRRC 24A WR beamline.

2. Experiment

The Er^{3+}-doped ZrO_2 films were obtained with various Er^{3+} concentrations using the sol–gel method. All chemicals, except the erbium (III) chloride ($ErCl_3$, anhydrous 99.9%, Strem Chemicals, Inc.), were reagent grade and were supplied by Aldrich, Inc. The doping of erbium (III) chloride was done with 0.5 mol%–6.0 mol%. Samples are called the undoped film, the 0.5 mol% dopant film, the 6 mol% dopant film, and so on. The samples were obtained using zirconium *n*-propoxide ($Zr(OPr)_4$) and erbium (III) chloride ($ErCl_3$) as precursors. All components were mixed in a solution of propanol (PrOH), acetylacetone (AcAc) and deionized water. After stirring at room temperature for 3 h, a clear precursor solution was obtained. A spin-coating procedure was adopted to deposit films on degreased fused-quartz substrates; these films were further sintered in an oven at controlled temperatures 1100 °C for 6 h, then cooled in an oven until room temperature.

The Photoluminescence (PL) experiments were conducted on ZrO_2 films that were irradiated with soft X-rays at the 24 A wide-range beamline in the third-generation 1.5 GeV storage ring at the National Synchrotron Radiation Research Center (NSRRC), Hsinchu, Taiwan. This beamline delivers photons with energies from 10 to 1500 eV [15]. Fig. 1 schematically depicts the system setup for the PL experiment. An incident focused and monochromatic soft X-ray photon flux was monitored using the photocurrent $I_0(E)$ derived from a copper mesh, which is placed in front of the sample. A photon energy of 300 eV was selected to excite the sample since this beamline had the highest photon flux in 300 eV. Then, the luminescence emission from the sample was focused using two lenses on the entrance slit of the monochromator. The PMT was applied to collect the photons from the exit slit of monochromator and then, the signal from the PMT was transferred to the multimeter for data acquisition using a computer. The PL measurements were made at room temperature using a monochromator from Acton Research Corporation (ARC) SpectraProTM VM-504, a 0.39 m triple grating, and a photomultiplier tube (PMT) R955 from Hamamatsu Photonics K. K, Japan. All PL spectra were normalized to the photon flux $I_0(E)$, and the X-ray diffraction (XRD) data were obtained at $\lambda = 1.5406$ Å using a Cu target at room temperature.

3. Results and discussion

Fig. 2 presents XRD data for ZrO_2 films doped with 0–6.0 mol% $ErCl_3$ on fused-silica substrates to elucidate how the dopant influences the host ZrO_2 structure. The films were obtained directly using the sol–gel method at a sintering temperature of 1100 °C. The background spectrum associated with fused-silica was subtracted from all data. The XRD spectrum of the undoped film reveals a pure monoclinic structure of ZrO_2 (ZrO_2/M), and the main peaks of $(\bar{1}11)_M$ and $(111)_M$ are at $2\theta = 28.34$ and 31.56 degree, respectively, based on PDF #36-0420, as presented in Fig. 2(a). However, the XRD spectrum of the ZrO_2 film with a high concentration, 6.0% of dopant, reveals a pure tetragonal structure of ZrO_2 (ZrO_2/T), and a main peak of $(101)_T$ at $2\theta = 30.50$ degree, according to PDF #81-1545, as displayed in Fig. 2(e). When the ZrO_2 film contained 2.0 mol% $ErCl_3$ dopant, as in Fig. 2(c), the XRD spectra exhibited not only the main monoclinic peaks of $(\bar{1}11)_M$ and $(111)_M$, and a strong peak at $2\theta = 28.97$ degree, but also a small tetragonal peak of $(101)_T$. The strong peak at $2\theta = 28.97$ degree corresponds to the cubic structure $(222)_C$ of Er_2O_3(Er_2O_3/C), according to the standard PDF #77-0463. As the concentration of Er^{3+} ions increases, the peaks of $(\bar{1}11)_M$ and $(111)_M$ diminish and the peak of $(101)_T$ increases. Then, the ZrO_2/T becomes dominant as the dopant concentration increases, further suggesting that Er^{3+} ions replace Zr^{4+} ions and cause a phase transition in host lattice of ZrO_2. Meanwhile, another crystalline phase of the cubic structure Er_2O_3/C was observed at a dopant concentration of 2 mol%, and the intensity of the peak of $Er_2O_3(222)_C$ then falls as the dopant concentration increases to 4 mol%. This result differs from that presented by Rosa-Cruz et al., [16], who found no Er_2O_3/C at dopant ion concentrations of 0.16–3.46 mol%.

Fig. 3 displays the photoluminescence (PL) spectra of ZrO_2 films that were doped with 0–6.0 mol% Er^{3+} ions on fused-silica substrates when the samples were excited with 300 eV soft X-rays. No PL emission peak was observed from the background of fused-silica substrates. For the undoped sample, the strong broad emission bands at around 400–600 nm centered at 485 nm with weak emission bands at 250–400 nm were observed. For the 0.5 mol% dopant film, not only were the main strong broad bands centered at approximately 485 nm and the weak bands at 250–400 nm observed, but also minor sharp peaks at around 500–570 nm and 650–700 nm appeared. For

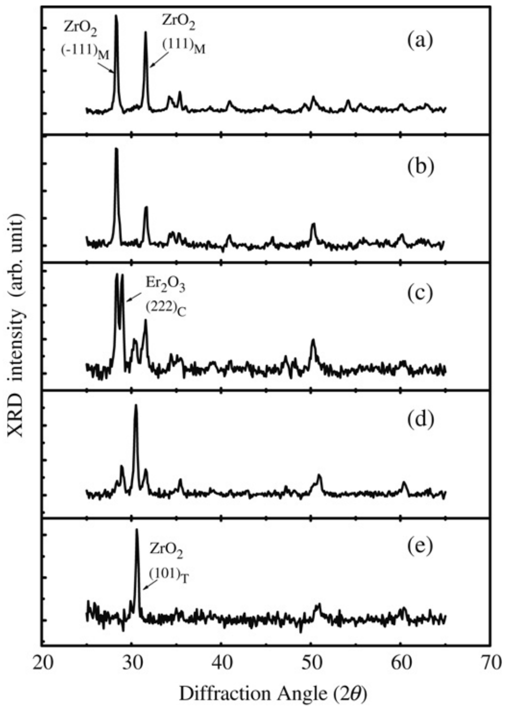

Fig. 2. XRD spectra of ZrO_2 films, with various mole concentrations of Er^{3+} ions. (a) 0 mol%; (b) 0.5 mol%; (c) 2.0 mol%; (d) 4.0 mol%; (e) 6.0 mol%.

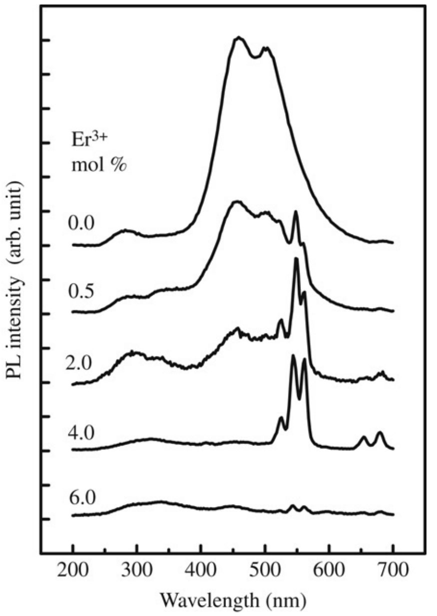

Fig. 3. PL spectra of ZrO_2 films doped with 0, 0.5, 2.0, 4.0 and 6.0 mol% of Er^{3+} ions, with excitation using 300 eV soft X-rays.

the 4 mol% dopant film, the main sharp peaks at 500–570 nm and 650–700 nm were clearly observed, but the minor peaks from 250 to 500 nm had almost disappeared. For the 6.0 mol% dopant film, the PL intensities, not only from 250 to 400 nm but also from 400 to 600 nm almost disappeared.

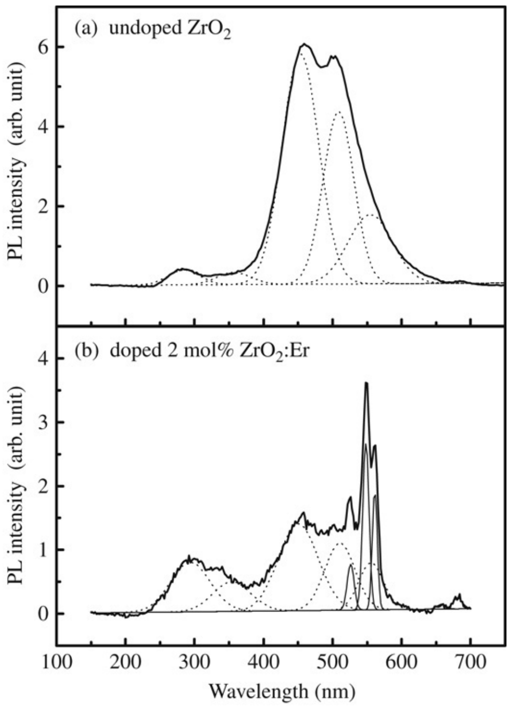

Fig. 4. Gaussian deconvolutions for the ZrO_2 films in Fig. 3. (a) Undoped ZrO_2 film; thick solid line: raw data, dashed line: fitted curves with the center peaks at around 290, 355, 450, 510 and 555 nm; (b) Doped 2.0 mol% film; thick solid line: raw data, dashed line: fitted curves with the broadened center peaks at around 290, 355, 450, 510 and 555 nm; thin solid lines: fitted curves with the sharp center peaks at around 525, 550, 560, 660 and 680 nm.

The PL spectrum from the samples can be fitted with Gaussian deconvolution as shown in Fig. 4. Fig. 4(a) displays the fitted curves with dashed lines from undoped ZrO_2 film, including the broadened center peaks at around 290, 355, 450, 510 and 555 nm. Fig. 4(b) presents the fitted curves from 2.0 mol% Er^{3+}-doped film, including not only the broadened center peaks, dashed lines, as undoped ZrO_2 film, but also the sharp center peaks, solid lines, at around 525, 550, 560, 660 and 680 nm. The main luminescence bands, centered at 485 nm, observed at 450, 510 and 555 nm from the undoped film are associated with the non-radiative relaxation of each electron, excited from the valence to the conductive band, to each luminescence recombination site and the subsequent luminescent relaxation from the luminescence recombination site to the valence band. This assumption is similar to that adopted by Rosa-Cruz et al. to account for the formation of the PL broad band centered at 490 nm [17]. However, the emission peaks at 290 and 355 nm from the undoped film are attributed to the radiative decay of self-trapped excitons (STE) and the capture of electrons by oxygen vacancies from the conduction band (CB), respectively. The results are similar to those of Kirm et al., [18] who found that the emission bands of the ZrO_2 film peaked at 4.3 and 3.5 eV, when the photon excitation energy exceeded 5.8 eV, which is the bandgap of ZrO_2. The sharp peaks from the 2.0 mol% doped film at 525 and 550–560 nm corresponds to the green emission band of the $^2H_{11/2} \rightarrow {}^4I_{15/2}$ and $^4S_{3/2} \rightarrow {}^4I_{15/2}$ of Er^{3+} transitions, respectively. However, the emission peaks at 660 and 680 nm are very weak, corresponding to the red emission band of the $^4F_{9/2} \rightarrow {}^4I_{15/2}$ of Er^{3+} transition.

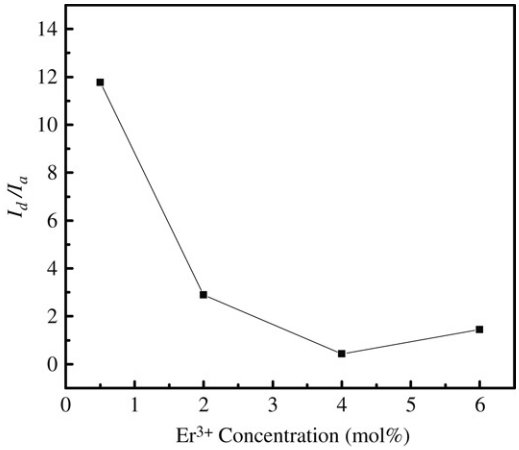

Fig. 5. PL intensity ratio for donor emission centered at 450 nm (I_d) to acceptor emission centered at 550 nm of Er^{3+}(I_a), corresponding to erbium ion dopant concentration.

The emission spectrum from the Er^{3+}-doped sample with a broad band centered at around 485 nm corresponds to the ZrO_2 host emission, and several emission lines that correspond to the erbium transitions, and proves that the energy transfer from the host to the active ions, was obtained. The host absorbs the energy, and then either emits the broad band that is centered at 485 nm or transfers its energy to Er^{3+} ions, which thus emit photons at various wavelengths. The emission band of the donor system, undoped ZrO_2, exhibits a greater fluorescence intensity than that of Er^{3+}-doped film. The lost energy is assumed to be associated with the transfer of non-radiation to the dopant, which in turn, after relaxation, generates the characteristic emission band of the active ion. Hence, the displayed emission bands of the Er^{3+} ion demonstrate the existence of the energy transfer from the host to the active ion. The increase in the ion concentration promotes the energy transfer process, increasing the fluorescent emission of the erbium ions and reducing the fluorescent emission of the host. This effect is revealed by evaluating the ratio of the fluorescent intensity of the donor system to that of the acceptor system. Fig. 5 displays the ratio of the donor emission centered at 450 nm to the acceptor emission centered at 550 nm. At higher dopant concentrations, the formation clusters are assumed to promote ion interaction and lead to the quenching of Er^{3+} fluorescence. This result is similar to that of Rosa-Cruz et al., concerning Sm^{3+}-doped ZrO_2 [17].

4. Conclusion

This work investigated the photoluminescence and crystalline structure of ZrO_2 and ZrO_2:Er^{3+}. Experimental results demonstrate a strong fluorescence emission broad band centered at 485 nm from the undoped ZrO_2 film. However, the Er^{3+}-doped ZrO_2 films exhibit not only a broad band centered at 485 nm, but also sharp characteristic bands, indicating that the ZrO_2 absorbs the energy, and then transfers it to Er^{3+}, the active ion, which then relaxes to produce the characteristic emission band of the active ion. Non-radiative energy transfer from the luminescence sites of the host to the active ion was performed. Also, the active ions stabilized the tetragonal phase of ZrO_2 and quenched the fluorescence emission of the host.

Acknowledgements

The authors would like to thank the National Synchrotron Radiation Research Center and the National Science Council of the Republic of China, Taiwan, (Contract No. NSC 93-2113-M-213-008) for financially supporting this research.

References

[1] J.V. Spirig, R. Ramamoorthy, S.A. Akbar, J.L. Routbort, D. Singh, P.K. Dutta, Sensors Actuators B 124 (2007) 192.
[2] M. Mamak, N. Coombs, G.A. Ozin, Chem. Mater. 13 (2001) 3564.
[3] A.S. Kao, G.L. Gorman, J. Appl. Phys. 67 (8) (1990) 3826.
[4] A.E. Bohé, J. Andrade-Gamboa, D.M. Pasquevich, A.J. Tolley, J.L. Pelegrina, J. Amer. Cera. Soc. 83 (2000) 755.
[5] P. Li, I.-W. Chen, J.E. Penner-Hahn, Phys. Rev. B 48 (1993) 10074.
[6] E. Pereyar-Perea, M.R. Estra-Yanez, M. Garcia, J. Phys. D: Appl. Phys. 31 (1998) L7.
[7] R. Reisfeld, M. Zelner, A. Patra, J. Alloy. Compd. 300–301 (2000) 147.
[8] A. Garcia-Murillo, C. Le Luyer, C. Dujardin, T. Martin, C. Garapon, C. Pedrini, J. Mugnier, Nucl. Instrum. Meth. A 486 (2002) 181.
[9] X. Liu, B. Liu, M. Gu, L. Xiao, X. Xu, Solid State Commun. 137 (2006) 162.
[10] A. Koch, C. Aven, P. Spanne, A. Snigirev, J. Opt. Soc. Amer. A 15 (1998) 1940.
[11] A. Patra, C.S. Friend, R. Kapoor, P.N. Prasad, J. Phys. Chem. B 106 (2002) 1909.
[12] N. Maeda, N. Wada, H. Onoda, A. Maegawa, K. Kojima, Thin Solid films 445 (2003) 382.
[13] R.I. Merino, J.A. Pardo, J.I. Peña, G.F. De La Fuente, A. Larrea, V.M. Orera, Phys. Rev. B 56 (1997) 10907.
[14] L.J. Lai, C.S. Su, J. Appl. Phys. 85 (1999) 8362.
[15] L.J. Lai, P.C. Tseng, Y.W. Yang, S.C. Chung, Y.F. Song, N.F. Cheng, C.C. Chen, C.T. Chen, K.L. Tsang, Nucl. Instrum. Methods. A 467–468 (2001) 586.
[16] E. De la Rosa-Cruz, L.A. Díaz-Torres, R.A. Rodríguez-Rojas, M.A. Meneses, O. Barbosa-García, P. Salas, Appl. Phys. Lett. 83 (2003) 4903.
[17] E. De la Rosa-Cruz, L.A. Díaz-Torres, P. Salas, R.A. Rodríguez-Rojas, G.A. Kumar, M.A. Meneses, J.F. Mosiño, J.M. Hernández, O. Barbosa-García, J. Appl. Phys. 94 (2003) 3509.
[18] M. Kirm, J. Aarik, M. Jürgens, I. Sildos, Nucl. Instrum. Methods. A 537 (2005) 251.